Influence of fibre reinforcement on the mechanical anisotropy of liquid crystal polymers

R. A. Chivers and D. R. Moore
ICI Wilton Materials Research Centre, PO Box 90, Wilton, Middlesbrough, Cleveland TS6 8JE, UK
(Received 19 December 1989; revised 19 July 1990; accepted 19 July 1990)

An evaluation of stiffness, toughness and strength has been performed on four materials based on thermotropic liquid crystalline polymers. These were of two different chemistries, with and without 27 wt% of short glass fibre. The change in chemistry had little effect on the stiffness properties, but the addition of glass fibre reduced the in-plane stiffness anisotropy. Laminate modelling was performed in an attempt to reproduce this. Fracture toughness also showed considerable anisotropy, both with and without glass, in the nature of the fracture surface and values obtained. Under long-term loading, the unreinforced material delaminated more severely than the glass fibre reinforced system, and also showed a transition in behaviour on dynamic loading.

(Keywords: anisotropy; liquid crystals; fibre)

INTRODUCTION

Main chain thermotropic liquid crystalline polymers (LCPs) are a relatively new class of materials. Chemically, they are polyesters in which the monomers are essentially aromatic: benzene and naphthalene units usually prevail, but a number of different systems have been considered[1]. Commercial applications of these polymers have mostly been based on their dimensional stability and ease of processing[2].

The unique feature of these polymers is that the molecules behave as rigid rods, this rigidity being conferred by the aromatic units and ester linkages. These molecules remain oriented in the melt, hence the name LCP. Orientation of rods in flowing melt leads to easy processability, but when the melt solidifies, in a mould or extruded sheet, the resulting orientation is retained[3]. This gives rise to a mechanical anisotropy in the component.

A number of studies have been devoted to this class of polymers. At the molecular level, X-ray diffraction has provided information on the randomness of the monomers in individual molecules[4] and this has led to consideration of how the molecules pack together and the nature of crystallites[5,6]. On a larger scale, electron microscopy on fracture surfaces of mouldings has shown the many different scales of fibrillar structure within the material[7,8]. Studies on such fibres have permitted the determination of some mechanical properties; tensile and torsional moduli of the polymer in its most basic form[9]. Any larger component will be made up of a number of basic fibrous units and the stiffness properties will reflect this orientation function more than the properties of the fundamental units[10]. Reference 10 suggests that the nature of the molecule is unimportant in the stiffness of the component aside from its influence on the ability to orient in the flow fields during processing.

Any characterization of the mechanical properties of these polymers is likely to depend on the nature of the processed components studied. The work reported here was performed on one specific injection moulding type, and it is therefore anticipated that properties determined are comparable and differences observed have resulted from real differences in the level of orientation adopted by the specific polymers and composites themselves.

It is well-known that the flow fields in the injection moulding process do not lead to a uniform isotropic orientation in the resulting component. When short glass fibres are present, then the orientation of these can be easily seen, and this can be used to map out the flow patterns. The nature of flow is such that the surfaces (skins) of the moulding are essentially aligned parallel to the main flow direction (i.e. into the component). In the centre (core), the alignment is not so good, but the basic direction is perpendicular to the flow (transverse across the width of the component but with some through-thickness orientation)[11]. Very similar effects have been observed in main-chain LCPs, in which the orientation of the rod-like molecules shows the flow without the need for any second constituent[10,12]. This has given rise to the term self-reinforcing polymers (SRP). Detailed studies of orientation in LCPs have shown that the skin layer (typically 1 mm thick in a 3 mm thick moulding) consists of a number of much thinner layers, each with a distinct net orientation and some degree of distribution of orientation[10]. These layers probably help to produce the very splintery nature of a typical fracture surface.

The principal aims of this paper are to describe macroscopic engineering properties for two LCPs and their short glass fibre reinforced composites. Although a thorough understanding of these materials is beyond the scope of this work, it is necessary to have some knowledge of their engineering properties for activities such as design feasibility studies. An understanding of the stiffness and fracture properties will be attempted, but a full account will inevitably occupy material scientists for a number of years yet. The aim of this paper is therefore to articulate

0032-3861/91/122190-09

the problems and to describe the engineering behaviour of some new materials.

EXPERIMENTAL

Materials

The LCPs used in this study have two different chemical compositions. Both polymers are random aromatic copolyesters. One system is based on *p*-hydroxybenzoic acid (HBA), isophthalic acid (IA) and hydroquinone (HQ) and is designated LCP1 (HBA/IA/HQ). The other system is based on *p*-hydroxybenzoic acid (HBA) and 2-hydroxy-6-naphthoic acid (HNA) and is designated LCP2 (HBA/HNA). Glass fibre reinforced versions of these plastics were also used where the glass content was 27% w/w. These materials are designated GF/LCP1 (HBA/IA/HQ) and GF/LCP2 (HBA/HNA).

All four materials were injection moulded under standard conditions in the form of square coathanger plaque mouldings ($150 \times 150 \times 3$ mm). The coathanger gate produces a straight flow front across almost the entire width of the mould tool. All specimens were cut from the uniform region, ignoring the extreme edges (*Figure 1*).

Techniques

A number of different techniques were used to evaluate the modulus of the samples. A lever loading creep machine[13] provided isochronous modulus and creep data in tension. An Instron universal test machine provided tensile modulus data from a ramp test at 2 mm min^{-1}. Lateral contraction ratios were measured in these tests using special extensometry[14]. Plate modulus ($E/1\text{-}\nu^2$) was determined on the entire coathanger plaques and from discs cut from the plaques using the techniques described by Stephenson *et al.*[15]. Isochronous shear modulus at small strains was obtained by the technique described by Bonnin *et al.*[16], using the geometric coefficients that are necessary to determine modulus from the torsional stiffness of rectangular prismatic specimens relating to isotropic materials, although recognizing that the LCP materials are anisotropic.

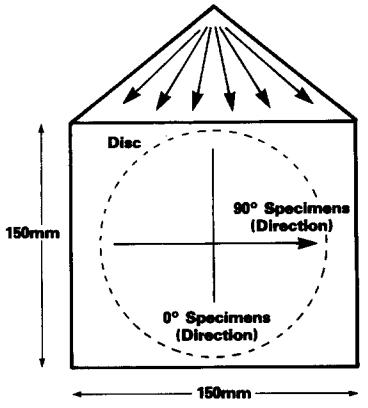

Figure 1 Diagram of the coathanger plaque moulding (3 mm thickness), showing the definition of the specimens used in this work. The directions 0° and 90° relate to stress directions

Fracture behaviour was determined in strength and toughness tests. Linear elastic fracture mechanics was adopted in the analysis of fracture of single edge notched flexure bars tested at 1 mm min^{-1} at −50°C. The European Group on Fracture protocol[17] was used as the basis of testing and analysis. Creep rupture and dynamic fatigue of unnotched specimens was conducted using the techniques described by Gotham[18]. The fatigue experiments were conducted at 0.5 Hz with a square waveform in a load control mode. Creep rupture and fatigue were conducted at 23°C.

Yield strength was determined by a uniaxial compression technique applied to small square specimens[19] where the axial force was applied through the plaque thickness (test speed 1 mm min^{-1} at 23°C).

STIFFNESS CHARACTERIZATION

Presentation of results

Injection mouldings are known to exhibit a layered structure as a consequence of the complex combinations of converging and diverging stress during the process of mould filling[11]. If the layers through the thickness of the moulding contain materials that can orient (long polymer chains or fibres) then the properties in one layer are likely to be different from those in the next layer. A complex anisotropy is likely to ensue in the plane of the moulding and through the thickness of the moulding. A full characterization of this anisotropy is bound to require a combination of mechanical property and morphological studies. For some materials, such studies have been conducted[20]. However, such an approach is beyond the scope of this paper. Nevertheless, a wide modulus characterization using tensile and bending load configurations can reflect certain aspects of this anisotropy.

Table 1 summarizes a range of values for small strain modulus at 23°C for the two LCPs and their short glass fibre reinforced composites. Although these results were obtained by a combination of step-load (constant load for 100 s) and ramp tests, it is unlikely that these minor differences in time dependence are influencing the comparisons of modulus. There may be some differences between modulus by tension (E) and plate modulus

Table 1 Summary of modulus for LCP plastics at 23°C

Type of modulus (GPa)	LCP1 (HBA/IA/HQ)		GF/LCP1 (HBA/IA/HQ)		LCP2 (HBA/HNA)		GF/LCP2 (HBA/HNA)	
	0°	90°	0°	90°	0°	90°	0°	90°
Tension								
E (100s, 0.2%)	14.1	–	13.5	–	12.4	–	15.1	–
E (2 mm min^{-1}, 0.5%)	13.6	2.1	14.7	4.0	–	–	–	–
Flexure								
$(E/1-\nu^2)$ Disc	14.0	1.7	13.2	3.3	12.3	2.1	13.5	3.0
$(E/1-\nu^2)$ Plaque	14.3	1.8	15.5	3.2	14.0	2.2	15.4	3.5

Table 2 Shear moduli and Poisson's ratios at 23°C

	LCP1 (HBA/IA/HQ)		GF/LCP1 (HBA/IA/HQ)		LCP2 (HBA/HNA)		GF/LCP2 (HBA/HNA)	
	0°	90°	0°	90°	0°	90°	0°	90°
Shear modulus (100s, 0.1%) (GPa)	1.14	–	1.57	–	1.09	–	1.29	–
Lateral contraction ratios (Poisson's ratios)								
Width	0.40	0.07	0.40	0.13	–	–	–	–
Thickness	0.45	0.67	0.50	0.66	–	–	–	–

$(E/1-\nu^2)$ by flexure, because the latter contains a $(1/1-\nu^2)$ term. Therefore when $\nu=0.4$ the tensile moduli will be 16% smaller than the plate moduli. If ν is very small (e.g. $\nu<0.1$) then the difference between the two moduli will be negligible. These differences between tensile and flexural properties relate to perfectly homogeneous samples. If the samples are heterogeneous, then further factors come into consideration.

A reference to 0° in *Table 1* implies a specimen cut along the direction of flow and/or stressed in the direction of flow, and 90° is a specimen cut or stressed perpendicular to this. This is shown in *Figure 1*. Several observations can be made from these modulus determinations.

(1) The LCP samples (LCP1 and LCP2) show considerable stiffness anisotropy. For example, the ratio of moduli in tension for the 0° and 90° directions for LCP1 is 6.7, and 8.0 in flexure.

(2) The higher stiffness anisotropy ratio in flexure compared with tension arises because of a lower 90° modulus in the flexural measurement. The modulus measurements for the 0° directions are generally similar between tensile and flexural loading modes.

(3) Glass fibre reinforcement of the LCPs has little reinforcing effect in the 0° direction. Modulus reinforcement in the 90° direction is significant i.e. up to a factor of two. Hence, the stiffness anisotropy ratio of the glass fibre reinforced materials is considerably less than that of the unreinforced polymers. For example, the ratio of moduli in tension for the 0° and 90° directions for GF/LCP1 is 3.4 (4.0 in flexure). This compares with 6.7 and 8.0, respectively, for LCP1.

Other stiffness characteristics are summarized in *Table 2* for shear properties and lateral contraction ratios.

The shear moduli are modestly enhanced by the addition of short glass fibres to the LCPs. However, the overall magnitude of shear modulus for these LCPs is similar to that for other conventional thermoplastics.

The lateral contraction ratios for 0° and 90° specimens measured in the width direction further illustrate the high stiffness anisotropy. The comparison of tensile modulus and plate modulus data in *Table 1* where the $1/(1-\nu^2)$ term is involved requires the width value of the lateral contraction ratio. The 0° modulus measured in flexure is therefore somewhat lower than that measured in tension, but the 90° modulus is little changed. A clearer description of the in-plane anisotropy of these mouldings is shown in *Figures 2* and *3* for the plate modulus *versus* angle between mould fill direction and applied stress. *Figures 2* and *3* show results for the LCP1 and LCP2 materials, respectively. In both cases, the glass fibre reinforced materials exhibit a broader modulus-direction distribution. In other words, the 'in-plane' anisotropy is less for the glass fibre composites and this is also reflected in the data for the Poisson's ratios (width measurements) in *Table 2* where the ratio of Poisson's ratios (0:90°) is less for the glass fibre reinforced materials.

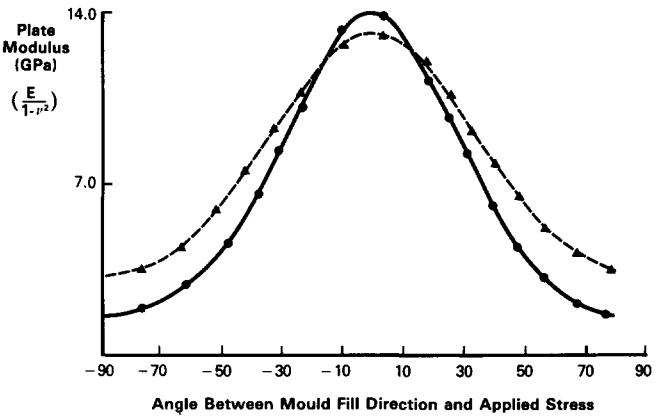

Figure 2 Disc stiffness at 23°C of LCP1 (●) and GF/LCP1 (▲) plotted against angle to the mould fill direction

Examination of isochronous stress *versus* strain curves for a plastic and its glass fibre reinforced composite can be revealing in terms of the bond between matrix and fibre. In *Figure 4*, the stress–strain plots of LCP2 and GF/LCP2 (i.e. the HBA/HNA materials) show that the curves are parallel for 0° specimens and that the addition of glass fibres to an LCP2 matrix provides some reinforcement. These curves are almost parallel, indicating that the modulus-strain function is very similar in both materials. This suggests that even as the deformation increases, the matrix remains well bonded to the glass. If bonding were poor, the glass fibres would separate and the polymer would act as if voided at high deformations, showing a reduced modulus.

Figure 5 for LCP1 and GF/LCP1 (i.e. the HBA/IA/HQ) material also shows parallel curves. This again indicates that the fibre matrix bond is apparently good, although on this occasion, the glass fibres confer no reinforcement in the mould fill direction (0° direction).

With these introductory comments, it is interesting to examine the creep behaviour of these four materials as shown in *Figure 6* for the LCP1 materials and *Figure 7* for the LCP2 materials. All creep curves are presented for 0° specimens at 23°C for a common short-term strain, achieved by the application of different applied stresses, since the moduli are different.

In *Figure 6*, it can be seen that the time dependence

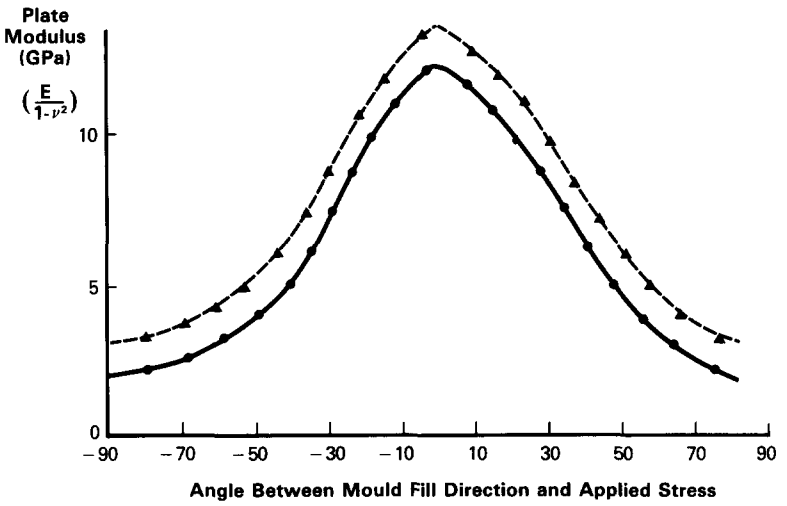

Figure 3 Disc stiffness at 23°C of LCP2 (●) and GF/LCP2 (▲) plotted against angle to the mould fill direction

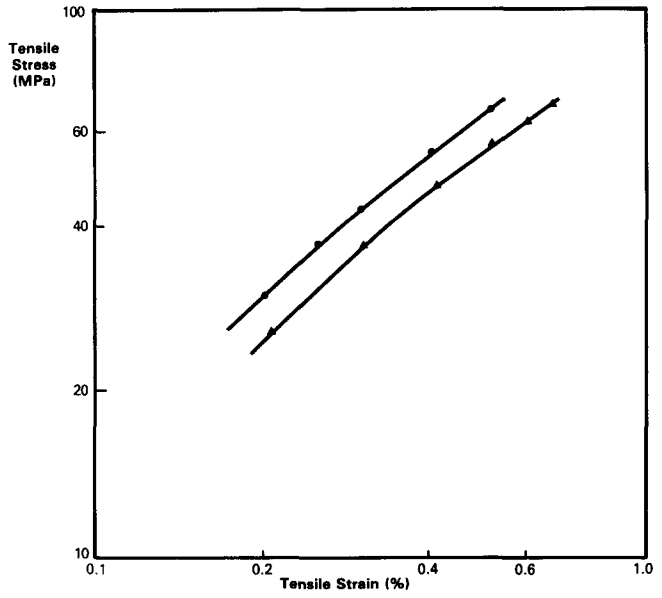

Figure 4 Tensile stress–strain (100 s) curves for LCP2 (▲) and GF/LCP2 (●), 0° specimens at 23°C

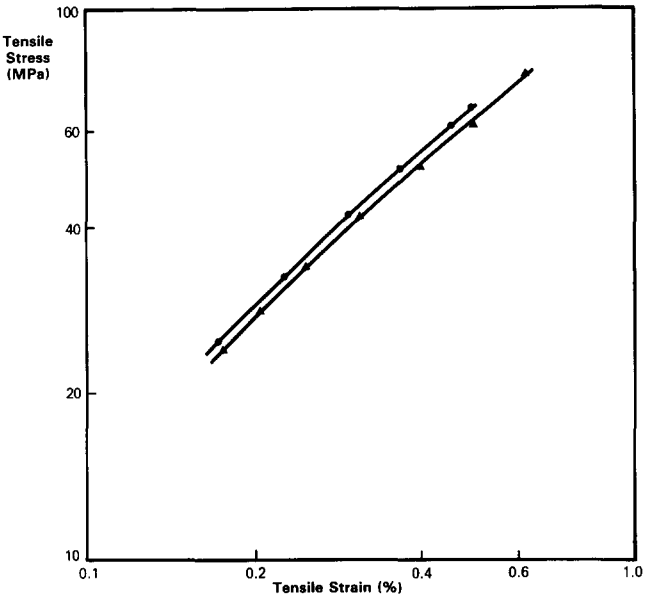

Figure 5 Tensile stress–strain (100 s) curves for LCP1 (●) and GF/LCP1 (▲), 0° specimens at 23°C

of modulus is less for GF/LCP1 than LCP1 (HPA/IA/HQ). Therefore, although the glass fibres do not confer stiffness reinforcement to the matrix at short times, they do at longer times. However, in *Figure 7* for the GF/LCP2 and LCP2 (HBA/HNA) a different picture emerges. The time dependence in modulus of the LCP2 is superior to that for its glass fibre reinforced composite. For these LCP2 materials, the addition of glass confers stiffness reinforcement at short times but this is eroded with time. Since there is some evidence of a good fibre/matrix bond at short times this suggests that the degree of viscoelasticity is quite low for the HBA/HNA plastics.

Further discussion on stiffness

The layered nature of injection mouldings can be modelled for stiffness by adopting a laminate theory approach[21,22]. This has been successful in predicting the stiffness of short glass fibre reinforced thermoplastics provided there is a knowledge of the orientation of the glass fibres in each layer, the fibre length distribution function and the component material properties [matrix tensile and shear modulus, fibre diameter and content, fibre tensile modulus and composite Poisson's ratio (lateral contraction ratio)]. Details of these calculations have been published previously[21] and are applied to the LCP materials and their composites. The calculations involve a number of assumptions and the use of the model is not to attempt a precise prediction of modulus but to picture the stiffness of the LCP materials conceptually.

For example, if the modulus in flexure for a glass fibre reinforced LCP composite in the 0° direction is required, it can be calculated on the basis of the following assumptions:

Matrix modulus = 8 Gpa
Fibre modulus = 76 GPa

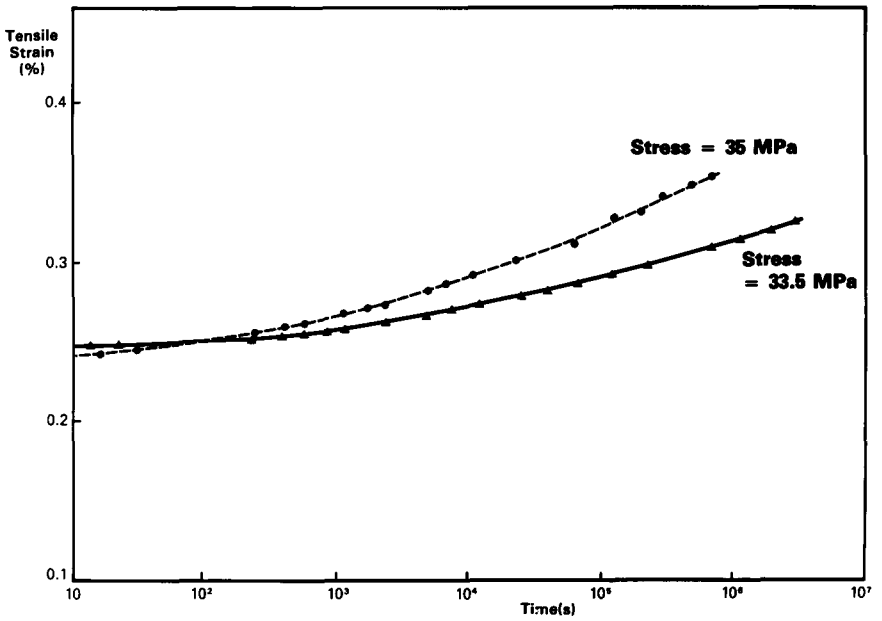

Figure 6 Tensile creep strain–time curves for LCP1 (●) and GF/LCP1 (▲) at 23°C

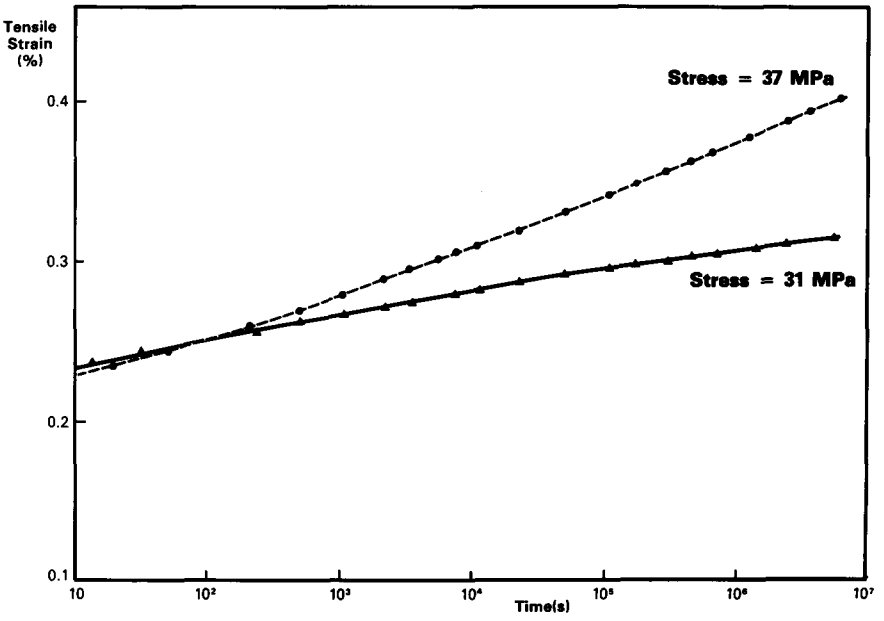

Figure 7 Tensile creep strain–time curves for LCP2 (▲) and GF/LCP2 (●) at 23°C

Shear modulus = 1 GPa
Fibre content 27% w/w (≡16% v/v)
Mean fibre length = 200 μm
Fibre diameter = 11 μm
Poisson's ratio of composite = 0.4
Orientation of fibres is 0° for 80% of thickness (skins) and 90° for 20% thickness (core)

A value of modulus in flexure in 0° direction for these parameters would be 13.8 GPa. (*Table 1* suggests a measured value of about 14 GPa.)

Most of these parameters are based on measurement. Only the orientation of the fibres and the matrix modulus are estimates. Since the polymer matrix itself is not isotropic, a single value close to the mean has been chosen, and it can be seen that a good overall modulus results. However, the degree of orientation chosen for the glass is clearly too high, so a lower orientation in the glass would be compensated for by a higher matrix orientation (and hence modulus). Conceptually, the model is working well, but a quantitatively accurate prediction is not necessarily expected.

Can the model conceptually account for the stiffness of the unreinforced liquid crystal polymers? The following parameters can be used in these laminate calculations:

Matrix tensile modulus = 3 GPa
Matrix shear modulus = 1 GPa
Modulus of oriented material = 100 GPa (ref. 10)
Volume of oriented material = 22 vol%
Diameter of oriented material = 2 μm
Orientation of oriented material (% of thickness) = 20% skin, random orientation; 20% core, 90° orientation; 60% intermediate layer between skin–core–0° orientation
Orientation length = 1000 μm

These assumed parameters are attempting to model the polymer as highly oriented fibres of length 1 mm, 2 μm diameter and volume fraction 22%, within a matrix of essentially totally unoriented polymer. There is no true observational basis for these assumptions. The calculated flexural modulus is 14 GPa, the same as that measured (*Table 1*).

The assumption of length for the oriented polymer chain is not critical because the same calculated modulus emerges for lengths above 1 mm. The apparent orientation, diameter and content is arbitrary. Nevertheless, the calculated modulus agrees with the measured modulus for this particular combination. So, if these assumptions were accurate, then the oriented chains would be acting as bundles rather than as individual chains, because individual chains would have a 'chain' diameter three or four orders of magnitude smaller.

These calculations are intellectually fanciful, but provide some interesting speculations of how to contemplate the consequence of the orientation in the LCPs. In part, they account for the lack of reinforcement of 0° modulus by addition of short glass fibres to the liquid crystal materials. Quite simply, the oriented polymer chains are stiffer than the glass fibres.

FRACTURE CHARACTERISTICS

Description of fractures

Three types of fracture tests have been conducted on these liquid crystal materials: notched fracture in a fracture mechanics test, and unnotched fracture in both creep rupture and dynamic fatigue tests. These relate to both 0° and 90° specimens. Naturally, much of the detail varies between each test and between the different conditions of testing. There is however, a first order similarity in the types of fracture.

Figure 8 shows the salient fracture patterns for 0° and 90° specimens and summarizes the qualitative features observed on the various fracture surfaces. For the 0° specimens, the core usually breaks at quite a distance from that position in the skin where the fracture started (this distance is marked 'x' in *Figure 8*). Consequently, the crack does not propagate at right angles to the stress direction all the way across the specimen. The layered structure through the thickness will account for this type of fracture as reported by Voss and Friedrich[23]. The quantitative strength data for the 0° specimens cannot therefore relate to a simple fracture mechanism.

The 90° specimens do not exhibit smooth fracture surfaces either, although to a first approximation the cracks run at right angles to the stress direction. Therefore, the quantitative data for the 90° specimens will be a closer approximation to a single fracture mechanism: cracking along the flow.

Overall, there is a clear observation of fracture anisotropy and multiple fracture mechanisms. A detailed study of the fracture characteristics would demand a combined mechanical and morphological approach, perhaps along the lines described by Voss and Friedrich[23].

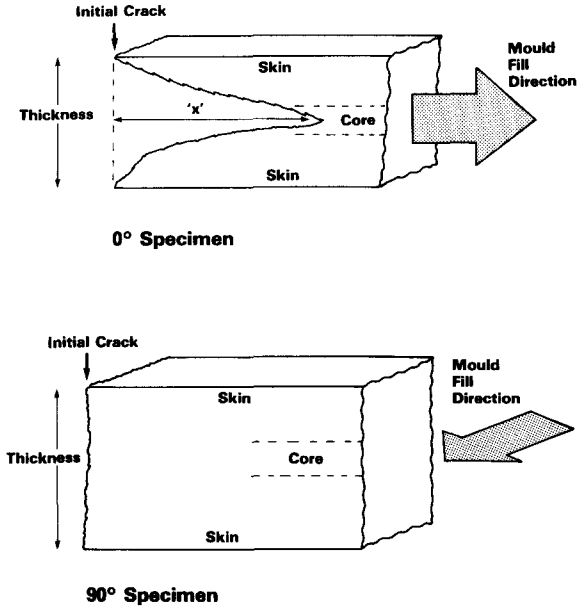

Figure 8 Illustration of typical fracture behaviour in the LCPs

Yield strength and fracture mechanics strength

Single edge notched bars were tested at −50°C at 1 mm min^{-1} in order to determine fracture mechanics strength K_{IC}. Yield strength (through the moulding thickness) was measured in compression at the same speed but at 23°C. Results for the four materials are summarized in *Table 3*.

The fracture mechanics data were tested for validity in terms of the size of the specimens and the form of the force–deflection curves that were obtained during fracture[17]. All the 0° specimens gave invalid fracture mechanics data. This was anticipated in the observations of the types of fracture discussed earlier. The 90° specimens are valid to a first approximation although clearly a micromechanical approach to these types of fracture would find difficulties in a simple application of linear elastic fracture mechanics theory.

Tensile yield strength is required to determine the size criteria for validity. Since these materials did not yield in tension, compressive tests were performed, which appeared to show yielding. Yield strength (σ_y) in compression can be converted to tensile yield strength by dividing by 1.3. Therefore, values of 51 MPa can be

Table 3 Fracture mechanics strength and yield for liquid crystal materials

	LCP1 (HBA/IA/HQ)		GF/LCP1 (HBA/IA/HQ)		LCP2 (HBA/HNA)		GF/LCP2 (HBA/HNA)	
	0°	90°	0°	90°	0°	90°	0°	90°
K_{IC} (−50°C)	6.2	2.0	5.6	3.3	10.0	3.8	8.9	4.1
Yield strength, $\sigma_{y,comp}$ (23°C) (MPa)	66		109		67		91	

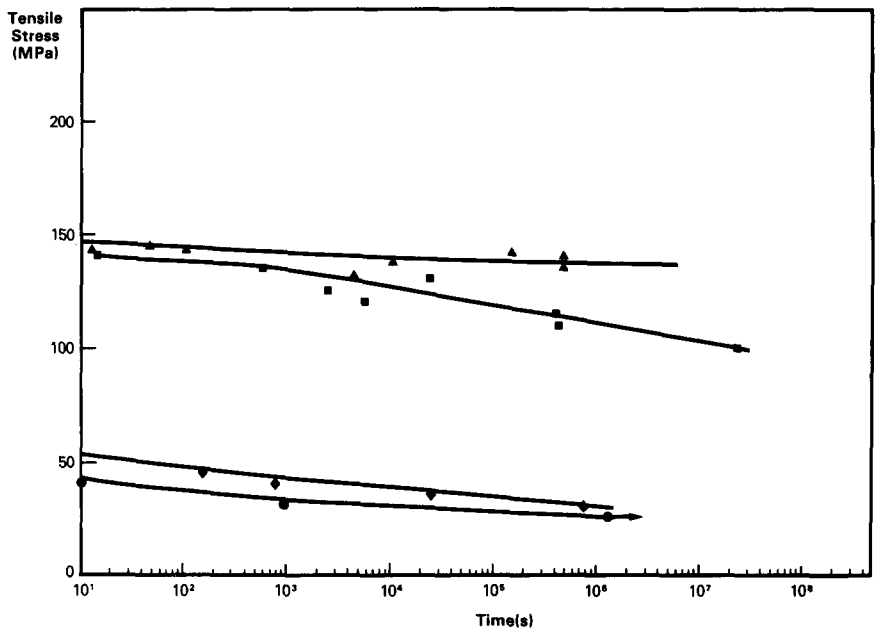

Figure 9 Creep rupture curves for LCP1 (▲,◆) and GF/LCP1 (■,●) at 23°C for both 0° (▲, ■) and 90° (◆, ●) specimens

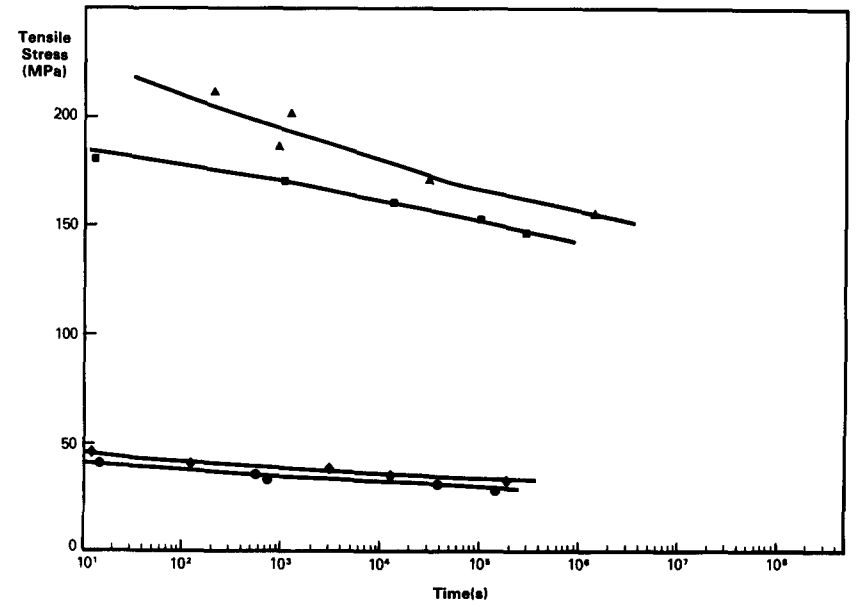

Figure 10 Creep rupture curves for LCP2 (▲,◆) and GF/LCP2 (■,●) at 23°C for both 0° (▲, ■) and 90° (◆, ●) specimens

expected for the tensile yield strengths of the unreinforced LCPs at 23°C. Yielding is naturally anisotropic in these materials, and the value determined here will be the lowest yield strength, giving the most conservative estimate for validity of the fracture mechanics data.

Creep rupture and fatigue

Strength under constant load (creep rupture) was measured on unnotched specimens of all four liquid crystal materials for 0° and 90° specimens. *Figure 9* shows the strength *versus* time under load curves for the LCP1 and GF/LCP1 materials and *Figure 10* shows these functions for the LCP2 and GF/LCP2 materials. The pattern of behaviour is similar. The difference between unreinforced and glass fibre reinforced polymers is small. The difference beween 0° and 90° is large. The difference between the 0° specimens based on LCP1 and LCP2 is also large.

The pattern of behaviour for the 90° specimens can be readily explained. The nature of the fractures is as described in *Figure 8*, i.e. fracture at approximately right angles to the stress field. The short-term (10 s under load) strength in creep rupture equates with the calculated yield strengths of the matrix materials (LCP1 and LCP2). Therefore the failure process for all the 90° specimens (unreinforced and glass fibre reinforced) is predominantly by a matrix yielding mechanism. This would seem to persist to long times under load since the curve of 90° strength *versus* time is relatively smooth, indicating no major transitions in the failure mechanism.

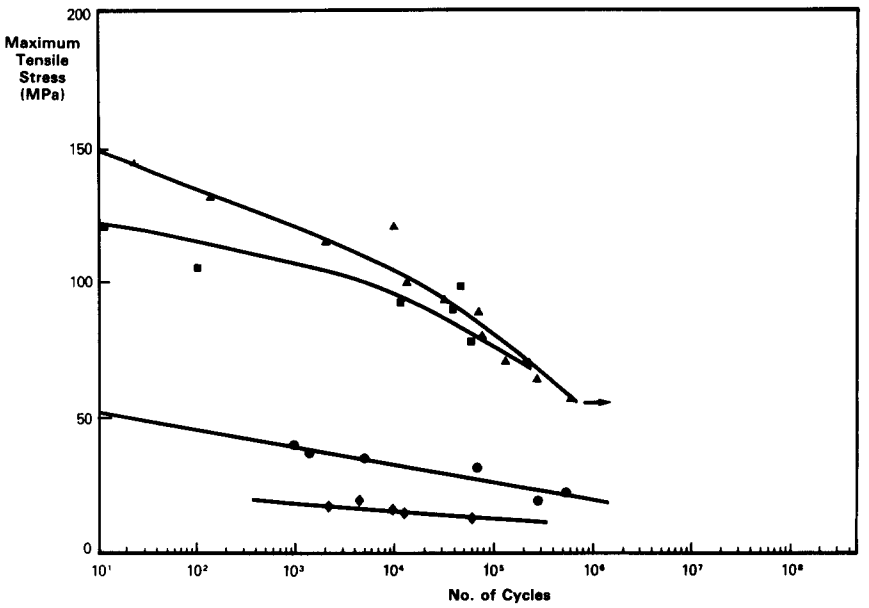

Figure 11 Dynamic fatigue stress–number of cycles curves for LCP1 (▲,◆) and GF/LCP1 (■,●) at 23°C for unnotched 0° (▲, ■) and 90° (◆, ●) specimens. Fatigue was conducted in zero-tension mode with a 0.5 Hz square waveform

The 0° specimens exhibit far higher strengths with a suggestion that the glass fibre reinforced compositions show slightly lower strength than the unreinforced materials. The failure mechanisms are complex and the fracture patterns are as described in *Figure 8*. The complexity of such fractures (and the absence of detailed morphological observations) prevents a simple account of these creep rupture functions. It would be, for example, unsupportable to suggest that fibre matrix debonding can account for the lower strengths of the glass fibre reinforced materials.

The dynamic fatigue behaviour of unnotched 0° and 90° specimens of LCP1 and GF/LCP1 is shown in *Figure 11*. The strength of the 90° specimens of the glass fibre reinforced material is now higher than that of the LCP1 material alone. It is likely that the cyclic nature of the stress field is introducing more crack-like behaviour into the matrix, and the glass fibres are then able to create more strength reinforcement. Certainly, the fracture strength of the LCP material alone is less than the yield strength of this matrix.

The 0° specimens in fatigue show much more time dependence than that observed in the creep rupture tests. There is also little difference between unreinforced LCP1 and glass fibre reinforced LCP1. The short-term strength (after 10 cycles) is the same as the short-term strength in creep rupture (i.e. after 10 s). Therefore, the initial failure processes can be expected to be the same. The long-term failure processes however are expected to be different in fatigue from those that occur in the static test, because the observed time dependence of strength is considerably different between the two tests.

Observation of the fracture surfaces helps to explain some of these trends in strength for the 0° specimens. In *Figure 8*, reference was made to the length 'x': the size of the 'tongue' in the 0° fracture surfaces. This distance characterizes the extent of delamination failure in the liquid crystal materials. These distances, 'x', have been measured approximately for the various materials in the various tests and are summarized in *Table 4* for the compositions based on LCP1.

Table 4 Values of 'x'–the fracture 'tongue' for 0° strength tests on LCP1 materials

	LCP1	GF/LCP1
Creep rupture		
High stress (short time)	Large (≈20 mm)	Small (≈5 mm)
Low stress (long time)	Large (≈15 mm)	Small (≈5 mm)
Fatigue		
High stress (small no. of cycles)	Large (≈15 mm)	Small (≈5 mm)
Low stress (large no. of cycles)	Small (≈5 mm)	Small (≈5 mm)

A large value of 'x' shows that delamination makes a major contribution to the failure of the specimen. The contribution of delamination is noticeably reduced when low stresses in fatigue occur for the unreinforced composition and when glass fibre reinforcement is present in the material. Transverse fracture also occurs and is similar to that observed for the 90° specimens and can either occur by yielding (as in creep rupture) or perhaps some crack-like fracture in the matrix (as in the fatigue case).

Therefore, the low stress fatigue experiments encourage both crack-like fracture in the transverse failure mode and a reduction in the extent of delamination damage (for both unreinforced and fibre reinforced material). This combination leads to an enhanced time dependence in fatigue strength compared with creep rupture strength. The ability of the matrix apparently to yield in the creep rupture tests on 0° specimens would seem to ensure a smaller time-dependence of strength in static tests.

CONCLUSIONS

The mechanical properties of a thermotropic liquid crystalline polymer, as of any fibre-reinforced system, depends on the particular moulded form of the material.

For a particular moulding type, we have characterized the bulk properties of stiffness, strength and toughness of two different polymers, both with and without short glass fibre reinforcement. A number of broad conclusions may be drawn.

(1) Considerable anisotropy of modulus in the plane of the moulding is present in all four systems. The anisotropy of the glass fibre reinforced polymers was less than that of the polymers alone, and calculations using a laminate model suggest that this is because 'fibres' of the polymer are stiffer than the glass fibres. In addition, we believe that the glass fibres disrupt the polymer orientation to some extent.

(2) The creep deformation behaviour of material with and without short glass fibre reinforcement is broadly similar, suggesting good fibre matrix bonding.

(3) Unreinforced polymer fails in static loading with considerable delamination in the skin and between the skin and core regions. With glass fibre reinforcement, this delamination is reduced. Under dynamic loading, there is a greater time dependence, with less delamination on testing at low stress for long times, but also reduced lifetimes compared with the same stress level applied statically.

(4) In notched fracture mechanics testing, considerable anisotropy is exhibited, with jagged failure and invalid results from 0° specimens and smoother surfaces and valid results from 90° specimens.

There is a need for further morphological studies to complement this work and explain the behaviour observed.

ACKNOWLEDGEMENT

The authors acknowledge the experimental measurements made by Barbara Slater, Julie Smith and Neil Witten.

REFERENCES

1 Chung, T. S. *Polym. Eng. Sci.* 1986, **26**, 901
2 Naitove, M. H. *Plast. Technol.* 1985, **85**, April
3 Ophir, Z. and Ide, Y. *Polym. Eng. Sci.* 1983, **23**, 792
4 Blackwell, J., Biswas, A., Gutierrez, G. A. and Chivers, R. A. *Faraday Discuss. Chem. Soc.* 1985, **79**, 73
5 Hanna, S. and Windle, A. H. *Polymer* 1988, **29**, 207
6 Biswas, A. and Blackwell, J. *Macromolecules* 1988, **21**, 3158
7 Sawyer, L. C. and Jaffe, M. *J. Mater. Sci.* 1986, **21**, 1897
8 Weng, T., Hiltner, A. and Baer, E. *J. Mater. Sci.* 1986, **21**, 744
9 Zachariades, A. N. and Porter, R. S. 'High Modulus Polymers. Approaches to Design and Development', Marcel Dekker, New York, 1988
10 Blundell, D. J., Chivers, R. A., Curson, A. D., Love, J. C. and MacDonald, W. A. *Polymer* 1988, **29**, 1459
11 Tadmor, Z. *J. Appl. Polym. Sci.* 1974, **18**, 1753
12 Menges, G., Schacht, T., Becker, H. and Ott, S. *Int. Polym. Proc.* 1987, **2**, 77
13 Dunn, C. M. R., Mills, W. H. and Turner, S. *Br. Plast.* 1964, July, 7
14 Barrie, I. T., Moore, D. R. and Turner, S. *Plast. Rubber Proc. Appl.* 1983, **3**, 365
15 Stephenson, R. C., Turner, S. and Whale, M. *Plast. Rubber Mater. Appl.* 1970, February, 7
16 Bonnin, M. J., Dunn, C. M. R. and Turner, S. *Plast. Polym.* 1969, December, 517
17 Williams, J. G. and Cawood, M. J. *Polym. Test.* 1990, **9**, 15
18 Gotham, K. V. *Plast. Polym.* 1969, August, 309
19 Davies, M. and Moore, D. R. *Comp. Sci. Technol.* 1990, 40
20 Ward, I. M. 'Mechanical Properties of Solid Polymers', 2nd Edn., John Wiley, Chichester, 1983, Ch. 10
21 Bailey, R. S., Davies, M. and Moore, D. R. *Composites* 1989, **20**, 453
22 Folkes, M. J. 'Short Fibre Reinforced Thermoplastics', Research Studies Press, Chichester, 1982
23 Voss, H. and Friedrich, K. *J. Mater. Sci.* 1986, **24**, 2889